



## Flow characteristics and drag reduction of tandem serial–parallel circular cylinders: a combined numerical and experimental study

W. Rauf\*<sup>1</sup>, M. Rifal<sup>1</sup>, R. Pido<sup>1</sup>, R.H. Boli<sup>1</sup>, N. Bumulo<sup>2</sup>

<sup>1</sup>Mechanical Engineering Department, Faculty of Engineering, Gorontalo University, Jl. Jl. Ahmad A. Wahab No. 247, Limboto, Gorontalo, 96214, Indonesia. Whatsapp +62 838 4651 9681

<sup>2</sup>Civil Engineering Department, Faculty of Engineering, Gorontalo University, Jl. Jl. Ahmad A. Wahab No. 247, Limboto, Gorontalo, 96214, Indonesia.

\*E-mail: wawan\_rauf@unigo.ac.id

### ARTICLE INFO

### ABSTRACT

#### Article History:

Received 29-02-2026

Accepted 30-03-2026

Available online 01-04-2026

#### Keywords:

Flow characteristics

Pressure coefficient ( $C_p$ )

Drag coefficient ( $C_d$ )

Computational

Experimental



*This study investigates the fluid flow characteristics and aerodynamic forces acting on three circular cylinders arranged in a tandem serial–parallel configuration using a combination of numerical simulations and experimental measurements. The spacing ratio between cylinders ( $N/D$ ) was varied from 0.1 to 1.1, while the Reynolds number ranged from 5,029.6 to 21,124.4. The numerical analysis was conducted using Computational Fluid Dynamics (CFD) to evaluate the flow structure and drag coefficient ( $C_d$ ), and the results were subsequently validated through experimental testing in a subsonic wind tunnel. The findings indicate that both the inter-cylinder spacing and the Reynolds number have a significant influence on wake structure, pressure distribution, and drag magnitude. At small  $N/D$  ratios, strong wake interactions between the cylinders generate extensive recirculation zones, low rear pressure, and high drag coefficients. As the  $N/D$  ratio increases, wake interference weakens, the flow becomes more orderly and symmetric, and the pressure distribution becomes more uniform, leading to a substantial reduction in drag. A consistent decrease in  $C_d$  with increasing Reynolds number is also observed for all configurations. The close agreement between numerical and experimental results demonstrates that the CFD approach accurately captures the flow behavior and aerodynamic forces. These findings provide valuable insights for optimizing tandem cylinder geometries in engineering applications, particularly for drag reduction and the enhancement of aerodynamic efficiency.*

## 1. INTRODUCTION

Fluid flow past vertically aligned circular cylinders arranged in a tandem configuration represents a geometric arrangement commonly encountered in structural and transportation engineering applications (Adeeb et al., 2018). Circular cross-section cylinders are widely employed in numerous engineering systems, including offshore structures, lighthouse towers, platform support components, and port facilities, as well as in heat transfer equipment such as shell-and-tube heat exchangers (Dawi et al., 2018., Dey et al., 2015., Ostapenko et al., 2017., Gabor., 2018). The interaction between structures and wind or water flows constitutes a critical design consideration that must be carefully addressed to ensure structural integrity and operational safety (Grioni et al., 2020).

Numerous previous studies have examined the flow characteristics around objects arranged in tandem configurations and their implications for aerodynamic drag (Salam et al., 2017., Qin et al., 2018). Among various geometries, circular cylinders are the most commonly adopted, particularly in land transportation systems such as trains and trailers, as well as in marine transportation applications including barge vessels (Liu et al., 2015). When cylinders are arranged sequentially in a serial-parallel configuration, the resulting wake interactions can significantly alter the flow pattern, thereby affecting pressure distribution, vortex intensity, and the magnitude of the aerodynamic forces acting on the system. Drag reduction strategies are generally implemented through flow field manipulation, one of which involves the placement of an additional element, known as an inlet disturbance body (IDB), upstream of the primary object to modify the incoming flow structure (Habiba et al., 2021). As fluid flows past tandem-arranged circular bodies, flow separation occurs along the surface and at the rear edges of the objects (Zhou et al., 2019), leading to energy losses within the boundary layer, a reduction in pressure recovery, and the generation of a pronounced pressure drag due to the substantial pressure difference between the front and rear surfaces (Tarakka et al., 2023., Habiba et al., 2023). In tandem serial-parallel arrangements, the flow passing the upstream cylinder experiences velocity deficits and wake formation, which subsequently interact with downstream cylinders. Such interactions may induce modifications in the flow structure, including shifts in separation points, wake contraction or expansion, and variations in vortex strength. These conditions can result in either beneficial effects, such as a reduction in total drag, or adverse effects, such as increased force fluctuations and flow-induced vibrations.

It is well established that wind and hydrodynamic loads acting on structures arranged in a group exhibit markedly different characteristics compared to those experienced by isolated structures of similar geometry (Liu et al., 2021). This behavior arises from complex interactions and combined flow disturbances around multibody configurations, which give rise to diverse and often unpredictable aerodynamic and hydrodynamic phenomena (Nguyen et al., 2018). Numerous studies have therefore focused on minimizing drag forces on both single cylinders and tandem cylinder arrangements using a wide range of flow control strategies. Despite the extensive body of research on fluid flow around isolated cylinders and cylinders arranged in purely series or parallel configurations, a comprehensive understanding of sequentially arranged serial-parallel circular cylinder configurations remains limited. Variations in inter-cylinder spacing, diameter ratio, and Reynolds number are known to play critical roles in governing flow behavior; however, the combined influence of these parameters on flow patterns and aerodynamic forces has not yet been fully elucidated.

Efforts to reduce drag forces through the use of drag-modifying bodies have been extensively investigated and implemented across various flow configurations. According to the findings of Etmianet et al., (2017.), when two circular cylinders are arranged in tandem and a T-shaped baffle plate with a head width of 5 mm is positioned upstream of the cylinders, the spacing between the plate and the cylinders plays a critical role in drag reduction. The optimal performance was achieved when the spacing-to-diameter ratio ( $L/D$ ) was within the range of 1.0 to 1.5.

Salam et al., (2020) reported a study on the influence of adding a cylindrical Inlet Disturbance Body (IDB) on the drag force acting on a square cylinder arranged in a tandem configuration, employing both computational fluid dynamics-based numerical simulations and experimental investigations conducted in a subsonic wind tunnel. The Reynolds number range examined was between 30,625 and 96,250. The diameter ratio between the IDB and the square cylinder ( $d/D$ ) was set to 0.08, 0.14, and 0.20, while the spacing ratio between the IDB and the square cylinder ( $L/D$ ) was varied from 0.0 to 1.0. The results demonstrated that increasing both  $L/D$  and  $d/D$  ratios contributed to reductions in the drag coefficient ( $C_d$ ) and pressure coefficient ( $C_p$ ). The maximum reduction in  $C_d$  reached 21.5962%, while the largest decrease in  $C_p$ , amounting to 14.7059%, occurred at  $L/D = 0.43$  and  $d/D = 0.14$ . In addition, Salam et al., analyzed flow separation characteristics for rectangular cylinders arranged in both series and parallel configurations. Their findings indicated that the minimum level of flow separation for both arrangements was achieved at a spacing ratio of  $M/D = 0.6$ .

Shui et al., (2021) evaluated drag reduction on a circular cylinder by installing an upstream disturbance element in the form of a drag rod. Their study demonstrated that both the diameter of the drag rod and the Reynolds number exert a significant influence on the flow pattern, with drag reductions of up to 63% being

achieved. For bodies with high blockage ratios, such as a flat plate positioned normal to the incoming flow, flow separation occurs directly at the plate edges and is largely independent of boundary-layer characteristics (Rauf et al., 2020). This research provides significant contributions to mechanical and civil engineering, particularly in the design of structures exposed to fluid flow such as towers, bridges, offshore platforms, and heat exchangers. The findings on spacing ratio effects improve aerodynamic efficiency, structural stability, energy performance, and mitigation of flow-induced vibration risks.

## 2. RESEARCH METHODS

The primary model investigated in this study consists of three circular cylinders of identical dimensions, as illustrated in Figure 1. This configuration is representative of various engineering structures, including multistory buildings, offshore structures, heat exchangers, and lighthouse towers. The study employs two complementary approaches, beginning with three-dimensional numerical simulations using Computational Fluid Dynamics (CFD) Fluent, followed by three-dimensional experimental validation. During the simulation stage, the test model was developed using Autodesk Inventor and placed within the computational domain, after which mesh generation was performed using Gambit 2.4.6, as shown in Figure 2. The numerical analysis focuses on flow characteristics and aerodynamic drag behavior. The specifications of the test model and the corresponding computational parameters are presented in Figure 3.

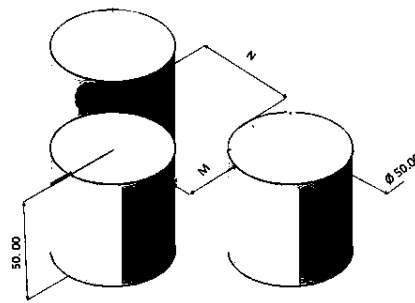
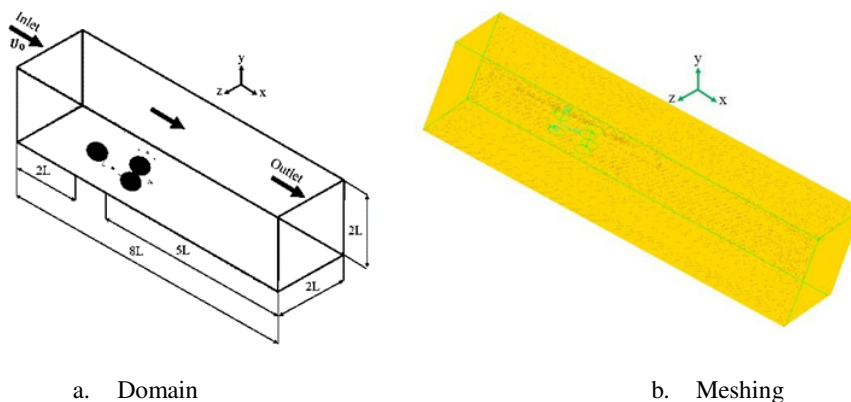


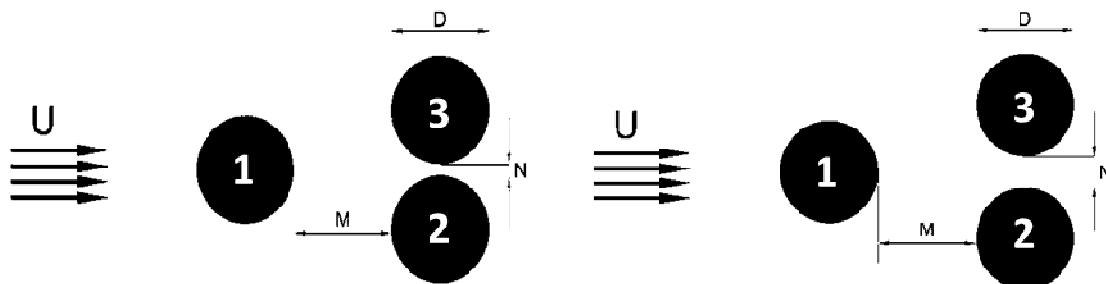
Figure 1. Test model



a. Domain

b. Meshing

Figure 2. Computation setup



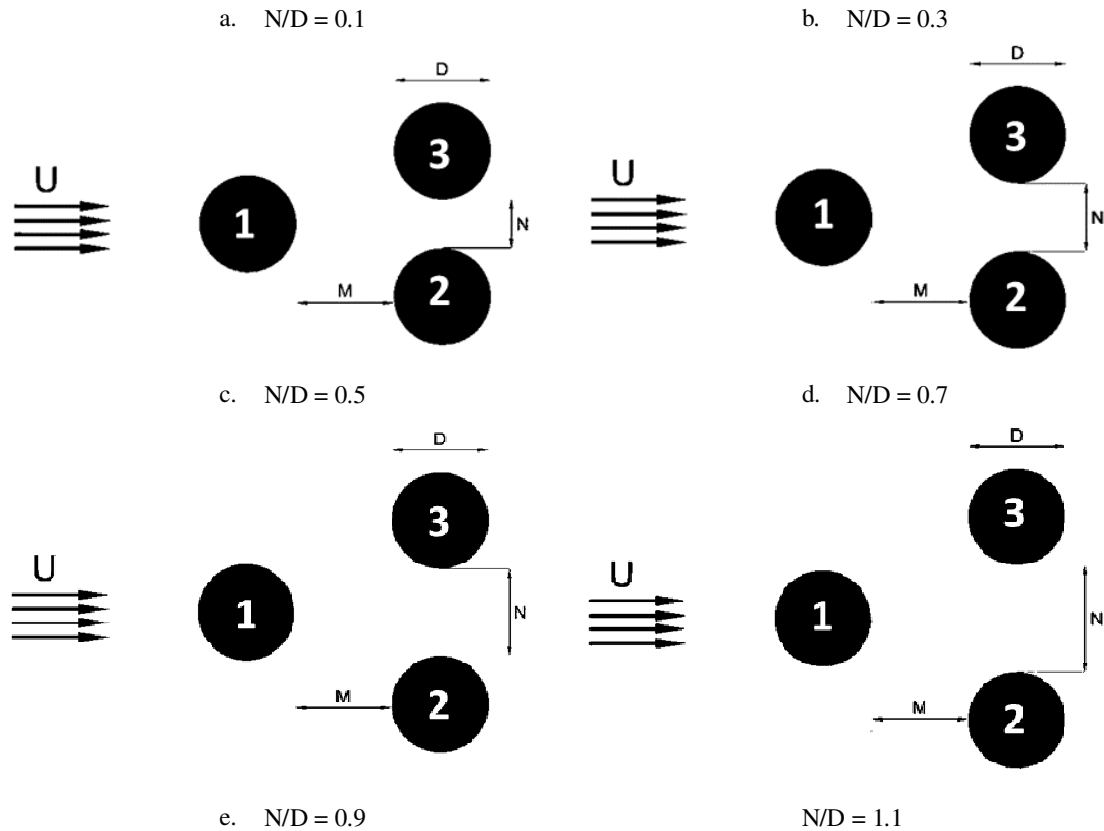


Figure 3. Test model specifications

The cylinder diameter ( $D$ ) was set to 0.05 m. The spacing between cylinder 1 and cylinders 2 and 3 was defined as  $M$ , while the spacing between cylinders 2 and 3 was defined as  $N$ . The distance  $M$  was kept constant at 0.05 m, resulting in a spacing ratio of  $M/D = 1$ . In contrast, the distance  $N$  was varied across six configurations, with values of 0.005 m, 0.015 m, 0.025 m, 0.035 m, 0.045 m, and 0.055 m, corresponding to  $N/D$  ratios of 0.1, 0.3, 0.5, 0.7, 0.9, and 1.1, respectively. For clarity, only selected cases ( $N/D = 0.1, 0.5,$  and  $0.9$ ) are presented in the flow visualization results from the experimental tests and in the flow characteristics obtained from the numerical simulations, as these spacing ratios are considered representative of the overall configurations.

The experimental investigation was conducted using a subsonic wind tunnel manufactured by Plint & Partners Ltd., Engineers, England, as shown in Figure 4. The test section was constructed from transparent acrylic with a thickness of 2.5 cm to facilitate flow observation during the experiments. The test model consisted of circular cylinders arranged in a tandem configuration, as illustrated in Figure 1. The cylinder length, width, and height were standardized based on the reference cylinder diameter ( $D = 0.05$  m), and all models were fabricated from acrylic material with a thickness of 2 mm. The inlet air velocity ( $U$ ) was varied from 7 to 21 m/s, resulting in Reynolds numbers of 5,029.6, 7,041.5, 9,053.3, 11,065.2, 13,077.0, 15,088.9, 17,100.7, 19,112.5, and 21,124.4.

During the experimental phase, the collected data included flow characteristics obtained through flow visualization techniques using the visualization apparatus shown in Figure 5, as well as pressure distribution and drag coefficient ( $C_d$ ) measurements. The dimensions of the experimental models were identical to those used in the numerical simulations. Drag force measurements were performed using a load-cell system directly connected to a computer. The force values recorded by the load cell were subsequently used to determine the drag force ( $F_d$ ) acting on the model, which was then expressed in nondimensional form as the drag coefficient ( $C_d$ ) using the following equation 1:

$$C_d = \frac{F_d}{\frac{1}{2} \rho v^2 A} \quad (1)$$

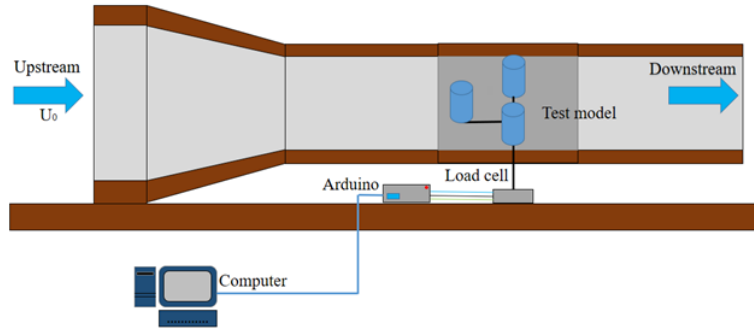


Figure 4. Experimental domain



Figure 5. Flow visualization tool

Pressure distribution measurements were focused on the entire circumference of the test model, as illustrated in Figure 6. For each cylinder, the pressure data obtained under different model configurations and Reynolds numbers were averaged to ensure accuracy and data reliability. The resulting pressure distribution was expressed in nondimensional form as the pressure coefficient ( $C_p$ ), which was calculated using the following equation 2:

$$C_p = \frac{P - P_0}{\frac{1}{2} \rho v^2} \quad (2)$$



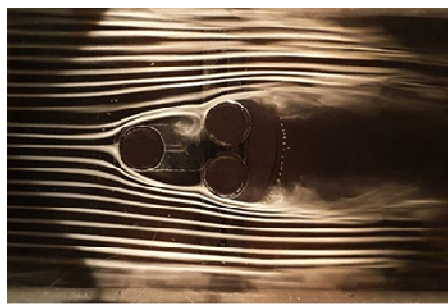
Figure 6. Pressure tap

### 3. RESULTS AND DISCUSSION

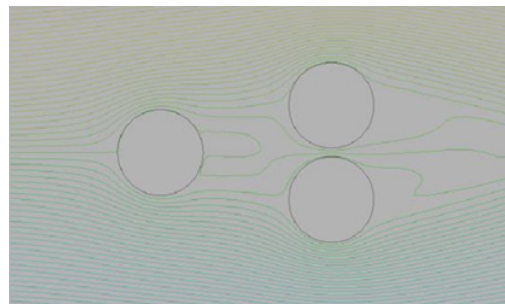
A comparison of flow characteristics obtained from flow visualization and numerical simulations for  $N/D$  ratios of 0.1, 0.5, and 0.9 is presented in Figure 7. For tandem cylinder arrangements, the flow behavior is strongly influenced by the inter-cylinder spacing ( $N/D$ ) and the Reynolds number ( $Re$ ). Flow visualization reveals that the first cylinder plays a dominant role in shaping the flow pattern around the second and third cylinders. At a small spacing ratio ( $N/D = 0.1$ ), the wake region behind the first cylinder remains highly energetic and directly impinges on the downstream cylinders. This interaction results in the formation of a large

and unstable recirculation zone, characterized by asymmetric streamlines and high vortex intensity. As the inter-cylinder spacing increases to  $N/D = 0.5$ , the wake generated by the upstream cylinder weakens before reaching the second and third cylinders. This behavior is indicated by a reduced separation region, more organized streamlines, and a decrease in vortex intensity downstream of the second cylinder. At larger spacing ratios ( $N/D = 1.1$ ), the flow around the second cylinder begins to resemble the flow characteristics of the first cylinder, although wake interaction effects remain detectable.

An increase in Reynolds number further contributes to changes in flow characteristics, as higher flow kinetic energy accelerates transition processes and alters the wake structure, thereby influencing pressure distribution and overall aerodynamic forces. In addition, when the second and third cylinders are closely spaced, a pronounced wake is generated, causing the flow to be deflected upward and leading to substantial boundary-layer growth. Introducing a finite  $N/D$  spacing between the second and third cylinders slightly delays flow separation and weakens the vortices formed downstream of the first cylinder. As a result, the boundary layer remains relatively thinner, and the vortices shed after passing the second and third cylinders are reduced in size. Under optimal spacing ratios, the wake patterns formed around tandem bodies promote a more streamlined flow, delaying separation and consequently reducing the drag coefficient of tandem-arranged structures (Shang., 2019).

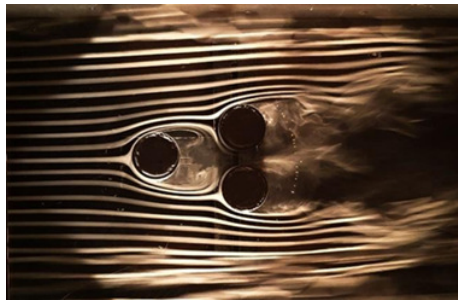


Visualization

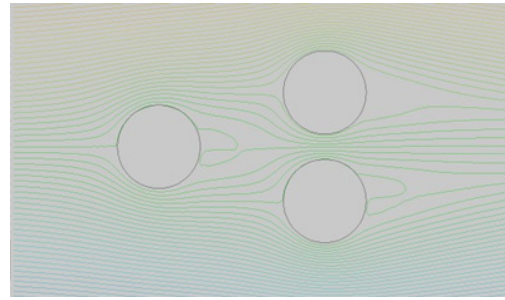


Computational

a.  $N/D = 0.1$



Visualization

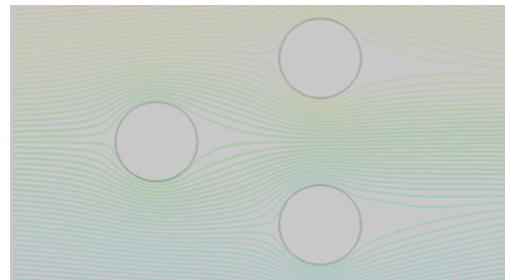


Computational

b.  $N/D = 0.5$



Visualization



Computational

c.  $N/D = 0.9$

Figure 7. Flow characteristics

Based on the data presented in Table 1, the average pressure coefficient ( $C_p$ ) was analyzed as a function of the Reynolds number ( $Re$ ) and the nondimensional spacing ratio ( $N/D$ ), which varied from 0.1 to 1.1. In general, all obtained pressure coefficient values are negative, indicating the dominance of suction effects on the model surface due to flow separation and the formation of a wake region downstream of the object. At  $N/D = 0.1$ ,  $C_p$  values range from  $-0.791$  to  $-1.058$  with increasing Reynolds number. The relatively small fluctuations observed at this spacing suggest that a closely spaced configuration provides a more stable pressure distribution with respect to changes in  $Re$ , indicating that flow interactions between the elements at this ratio do not yet produce significant disturbances.

For  $N/D = 0.3$ , the average pressure coefficient exhibits a gradual increasing trend in magnitude with increasing Reynolds number, reaching a minimum value of  $-1.005$  at  $Re = 19,112.5$ . The enhancement of negative pressure under this condition suggests an intensification of flow separation effects as a result of the larger inter-element spacing compared to the  $N/D = 0.1$  configuration. At intermediate spacing ratios ( $N/D = 0.5$  and  $0.7$ ), the average pressure coefficient consistently shows higher magnitudes, with minimum values of  $-1.239$  and  $-1.173$ , respectively. These results indicate that the inter-cylinder spacing at these ratios promotes more complex flow interactions, including vortex strengthening and wake expansion, leading to a more pronounced pressure reduction over the model surface.

At  $N/D = 0.9$ , a significant increase in the magnitude of the pressure coefficient is observed, particularly at  $Re = 17,100.7$ , where  $C_p$  reaches  $-1.39352$ , the lowest value among all tested configurations. This finding suggests that the combination of relatively large spacing and intermediate Reynolds numbers produces the most unfavorable pressure distribution due to intensified vortex activity and flow instability in the wake region. For the largest spacing ratio ( $N/D = 1.1$ ), the average pressure coefficient remains consistently high, with values ranging from  $-0.895$  to  $-1.290$ . Although this configuration does not always yield the absolute minimum  $C_p$ , it demonstrates that increasing the inter-cylinder spacing continues to contribute to the enlargement of low-pressure regions as the shielding effect between the cylinders weakens and the wake develops more freely.

Overall, these results indicate that both the Reynolds number and the  $N/D$  ratio exert a significant influence on the characteristics of the average pressure coefficient. An increase in the  $N/D$  ratio generally enhances the magnitude of negative pressure up to a certain optimal condition, beyond which a stabilizing trend is observed. These findings underscore the critical role of geometric configuration in controlling pressure distribution and flow behavior, which is highly relevant for aerodynamic design optimization and drag reduction strategies (Tarakka et al., 2021).

Table 1. Comparison of pressure coefficients

Re	Average pressure coefficient					
	N/D = 0.1	N/D = 0.3	N/D = 0.5	N/D = 0.7	N/D = 0.9	N/D = 1.1
5029.6	-0.944	-0.541	-0.756	-0.937	-0.92708	-1.093
7041.5	-0.944	-0.555	-0.979	-1.131	-0.77083	-0.895
9053.3	-1.048	-0.861	-1.194	-1.173	-1.13194	-1.173
11065.2	-0.791	-0.633	-1.223	-1.138	-0.79583	-1.070
13077.0	-0.809	-0.633	-1.003	-1.109	-0.83929	-1.159
15088.9	-0.929	-0.710	-1.033	-1.010	-1.13281	-1.247
17100.7	-1.033	-0.795	-1.012	-1.036	-1.39352	-1.206
19112.5	-0.983	-1.005	-1.239	-1.087	-1.23438	-1.272
21124.4	-1.058	-0.944	-1.112	-1.154	-1.21389	-1.290

Based on the numerical simulation results presented in Table 2, the drag coefficient ( $C_d$ ) exhibits a consistent decreasing trend with increasing Reynolds number for all variations of the nondimensional spacing ratio ( $N/D$ ). This trend indicates that enhanced fluid inertia reduces the contribution of pressure drag associated with flow separation in the wake region behind the model. At  $N/D = 0.1$ , the computed  $C_d$  values are the highest among all configurations. This behavior correlates with the pressure coefficient distribution, which reveals a

relatively narrow yet elongated low-pressure region, as well as with flow visualizations showing a confined wake with strong recirculation. Under these conditions, pressure drag dominates due to the pronounced pressure difference between the upstream and downstream sides of the model.

As the  $N/D$  ratio increases to 0.5 and 0.7, the computed  $C_d$  values decrease significantly. This reduction is consistent with the pressure coefficient results, which indicate a more uniform distribution of negative pressure along the model surface. Numerical flow visualizations at these spacing ratios reveal more organized vortex structures and a relatively stable wake, thereby mitigating energy losses associated with flow separation. At the largest spacing ratios ( $N/D = 0.9$  and  $1.1$ ), the computed  $C_d$  reaches its minimum values. Although the pressure coefficient exhibits large negative magnitudes, the more homogeneous pressure distribution and the increased wake symmetry contribute to a reduction in the overall drag force. These results demonstrate that the computational approach effectively captures the primary mechanisms of drag reduction through flow-structure control in the downstream region.

Table 2. Computational drag coefficients

N/D	Re								
	5029.6	7041.5	9053.3	11065.2	13077.0	15088.9	17100.7	19112.5	21124.4
0.1	1.4524	1.331	1.2622	1.2198	1.1892	1.1608	1.1414	1.1268	1.1162
0.3	1.3323	1.1986	1.1271	1.0778	1.0445	1.0196	0.9928	0.9843	0.9713
0.5	1.247	1.1182	1.0444	0.9958	0.9631	0.938	0.9186	0.903	0.8901
0.7	1.1859	1.0577	0.9894	0.9444	0.8975	0.887	0.8681	0.8527	0.8416
0.9	1.1393	1.0156	0.9496	0.9043	0.8721	0.8484	0.8304	0.8159	0.8042
1.1	1.0925	0.9728	0.9101	0.8641	0.834	0.8108	0.7934	0.7787	0.7676

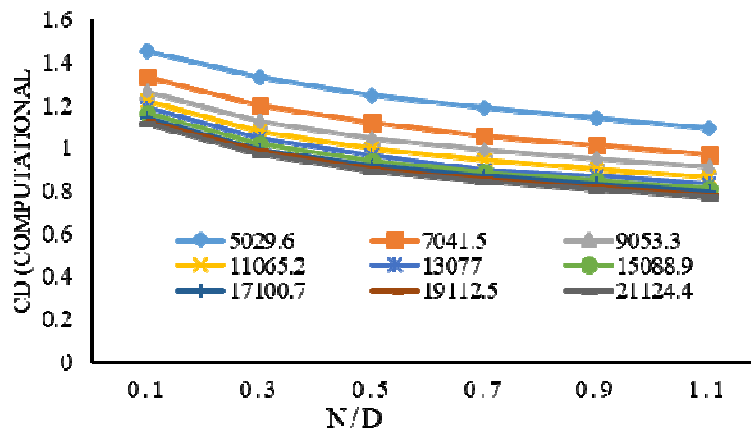


Figure 8. Comparison of drag coefficients for each  $N/D$  spacing ratio obtained from numerical simulations

The experimental results presented in Table 3 exhibit trends similar to those obtained from the numerical simulations, namely a reduction in the drag coefficient ( $C_d$ ) with increasing Reynolds number across all  $N/D$  ratios. However, the experimentally measured  $C_d$  values are generally slightly lower than the numerical predictions, particularly at intermediate to high Reynolds numbers. At  $N/D = 0.1$ , the experimental  $C_d$  values remain relatively high and display larger fluctuations compared to the numerical results. This behavior can be attributed to the influence of real-flow instabilities, non-ideal boundary conditions, and more pronounced turbulent fluctuations inherent in physical experiments. Experimental flow visualizations reveal a less stable wake than that observed in the numerical simulations, which directly enhances the contribution of pressure drag.

For  $N/D$  ratios ranging from 0.3 to 0.7, the experimental  $C_d$  values decrease in a more systematic manner. This trend is consistent with experimental flow visualizations showing more controlled vortex formation and a contraction of the wake region. The agreement between these trends and the pressure coefficient results indicates that a more uniform pressure distribution over the model surface plays a crucial role in reducing aerodynamic drag. At  $N/D = 0.9$  and  $1.1$ , the experimental  $C_d$  values reach their minimum levels. Flow visualizations under

these conditions show a wider yet relatively symmetric wake, with reduced vortex fluctuations compared to lower spacing ratios. Despite some data variability due to three-dimensional effects and inherent turbulence, the overall trend of drag reduction is preserved, confirming the effectiveness of the geometric configuration in mitigating drag forces.

Table 3. Experimental drag coefficients

N/D	Re								
	5029.6	7041.5	9053.3	11065.2	13077.0	15088.9	17100.7	19112.5	21124.4
0.1	1.3576	1.2753	1.1914	1.1825	1.1654	1.081	1.045	1.0516	1.0930
0.3	1.2655	1.1606	1.0603	1.0373	1.0064	0.9881	0.9694	0.9539	0.9412
0.5	1.2113	1.0913	0.9950	0.9313	0.9394	0.903	0.8940	0.8801	0.8700
0.7	1.154	0.9947	0.9501	0.9146	0.8671	0.867	0.8305	0.8349	0.8242
0.9	1.1156	0.9738	0.9096	0.8704	0.8539	0.8235	0.7933	0.798	0.7828
1.1	1.0019	0.9244	0.8307	0.8436	0.8003	0.761	0.7297	0.7582	0.7478

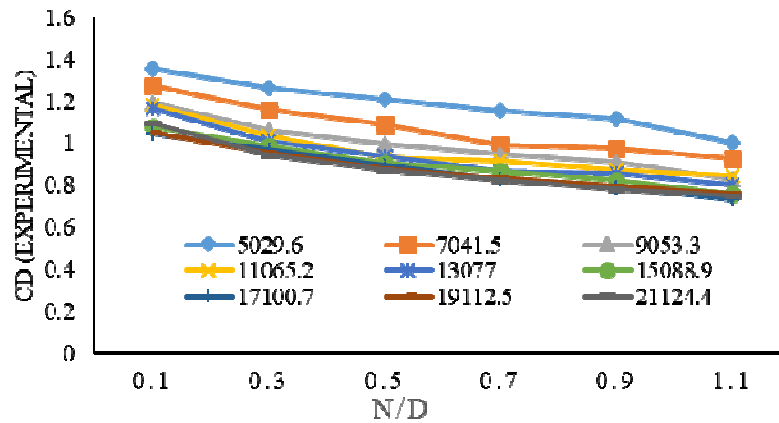


Figure 9. Comparison of the drag coefficient at each  $N/D$  spacing under experimental conditions

The discrepancies between the computational and experimental results are primarily attributed to the idealized assumptions adopted in the numerical simulations, such as the turbulence modeling approach and the application of uniform boundary conditions, in contrast to the experimental conditions that are inherently influenced by real-flow instabilities and three-dimensional effects. Nevertheless, the strong agreement in overall trends between both methods demonstrates that the computational approach exhibits good validity in predicting drag characteristics and flow patterns. From a physical perspective, both computational and experimental findings confirm that the reduction in the drag coefficient is closely associated with the pressure coefficient distribution and the downstream flow behavior. Configurations with larger  $N/D$  ratios promote a more uniform pressure distribution and a more stable wake structure, thereby effectively reducing the overall contribution of pressure drag (Wang et al., 2018).

#### 4. CONCLUSION

This study successfully provides a comprehensive investigation of fluid flow characteristics, pressure coefficient ( $C_p$ ) distributions, and drag coefficient ( $C_d$ ) behavior for a three-cylinder model arranged in a tandem configuration using a combined approach of numerical computation (CFD) and experimental testing. The results demonstrate that the inter-cylinder spacing ratio ( $N/D$ ) and the Reynolds number ( $Re$ ) are the primary parameters governing flow interaction, wake structure, and the overall aerodynamic performance of the system. From a physical standpoint, configurations with small  $N/D$  ratios generate strong wake interactions, extensive recirculation zones, and high vortex intensity, leading to reduced base pressure and increased drag coefficients. In contrast, increasing the inter-cylinder spacing to  $N/D$  values of 0.7–1.1 effectively weakens wake interference, enhances flow regularity, and produces more stable and symmetric wake structures. These conditions directly

contribute to pressure recovery and a significant reduction in the total drag force. The pressure coefficient analysis indicates that increasing  $N/D$  generally intensifies negative pressure levels up to an optimal condition, beyond which the trend becomes relatively stable. Meanwhile, both computational and experimental results consistently reveal a decrease in the drag coefficient with increasing  $N/D$  and  $Re$ , confirming that geometric arrangement of tandem cylinders represents an effective strategy for aerodynamic drag control. The strong agreement in trends between numerical predictions and experimental measurements further validates the reliability of the computational approach in capturing flow characteristics and aerodynamic forces in tandem cylinder configurations. Overall, this research confirms that optimizing inter-cylinder spacing in tandem arrangements enables effective control of flow interactions, modification of wake structures, and substantial drag reduction through pressure distribution management. This research reveals new wake interaction mechanisms and optimal spacing effects on drag reduction in three-cylinder configurations, while previous studies were limited to single- and two-cylinder arrangements.

#### ACKNOWLEDGMENTS

The authors gratefully acknowledge the Institute for Research and Community Service, Universitas Gorontalo, for providing financial support for this research. The authors also extend their sincere appreciation to the Head of the Mechanical Engineering Laboratory, Universitas Gorontalo, for providing the facilities and technical support necessary to conduct this study.

#### NOMENCLATURE

$C_d$	: Drag coefficient
$C_p$	: Pressure coefficient
$Re$	: Reynolds
$D$	: Diameter (m)
$P$	: Test pressure (Pa)
$P_0$	: Atmospheric pressure (Pa)
$\rho$	: Density ( $\text{kg/m}^3$ )
$v$	: Velocity (m/s)
$A$	: Area ( $\text{m}^2$ )

#### REFERENCES

- Adeeb, E., Haider, B.A., Sohn, C.H., Flow interference of two side-by-side square cylinders using IB-LBM – Effect of corner radius, *Results in Physics*, 10, 2018.
- Dawi, A.H., Akkermans, R.A.D., Direct and integral noise computation of two square cylinders in tandem arrangement, *Journal of Sound and Vibration*, 14, 2018.
- Dey, P., Das, A.K., Steady flow over triangular extended solid attached to square cylinder – A method to reduce drag, *Ain Shams Engineering Journal*, 2015.
- Etminan, A., Moosavi, M., Ghaedsharafi, N., Characteristics of aerodynamics forces acting on two square cylinders in the streamwise direction and its wake patterns, *Advances in Control, Chemical Engineering, Civil Engineering and Mechanical Engineering*, ISBN: 978-960-474-251-6, 2017.
- Gabor, O.S., Numerical study of the circular cylinder in supersonic ground effect conditions, *International Review of Aerospace Engineering (I.R.E.A.S.E)*, 1-12, 2018.
- Griani, M., Elaskar, S.A., Mirasso, A.E., A numerical study of the flow interference between two circular cylinders in tandem by scale-adaptive simulation model, *Journal of Applied Fluid Mechanics*, 13(1), 169-183, 2020.
- Habiba, H., Salam, N., Tarakka, R., Jalaluddin., Ihsan, M., Distribution of fluid flow pressure through tandem square cylinders with the addition of triangular cylinder as a disturbance object, *IOP Conf. Series: Earth and Environmental Science*, 841, 2021.
- Habiba, S., Salam, N., Tarakka, R., Jalaluddin., Ihsan, M., The effect of size ratios of the triangular disturbance cylinder to the square cylinder to the flow drag of tandem objects, *International Journal of Engineering and Science Applications*, 2023.
- Ostapenko, A., Bulanchuk, G., Calculations of the drag coefficient of circular, square and rectangular cylinders using the lattice Boltzmann method with variable lattice speed of sound, *Springer*, 2017.
- Salam, N., Tarakka, R., Jalaluddin., Bachmid, R., The effect of the addition of inlet disturbance body (idb) to flow resistance through the square cylinders arranged in tandem, *International Review of Mechanical Engineering (I.R.E.M.E.)*, 11(3), 181-190, 2017.

- Qin, B., Alam, M.M., Zhou, Y., Free vibrations of two tandem elastically mounted cylinders in crossflow, *J. Fluid Mech*, 861,394-381, 2019.
- Liu, M., Xiao, L., Yang, L., Experimental investigation of flow characteristics around four square-cylinder arrays at subcritical Reynolds numbers, *Int. J. Nav. Archit. Ocean Eng*, 7, 906-919, 2015
- Liu, Z., Zhao, W., Wan, D., CFD study of wave interaction with single and two tandem circular cylinders, *Ocean Engineering*, 239, 1-22, 2021.
- Nguyen, V.T., Chan, W.H.R., Nguyen, H.H., Numerical investigation of wake induced vibrations of cylinders in tandem arrangement at subcritical Reynolds numbers, *Ocean Engineering*, 154, 341-356, 2018.
- Rauf, W., Tarakka, R., Jalaluddin, Ihsan, M., Effect of flow separation control with suction velocity variation: study of flow characteristics, pressure coefficient, and drag coefficient, *Universal Journal of Mechanical Engineering*, 8(3), 142-151, 2020.
- Salam, N., Tarakka, R., Jalaluddin, Ihsan, M., Flow separation across three square cylinders arranged in serial and parallel tandem configuration, *IREA*, 8(3), 2020
- Shang, J., Zhou, Q., Alam, M.M., Liao, H., Cao, S., Numerical studies of the flow structure and aerodynamic forces on two tandem square cylinders with different chamfered-corner ratios, *Physics of Fluids*, 31, 1-16, 2019.
- Shui, Q., Duan, C., Gu, Z., New insights into numerical simulations of flow around two tandem square cylinders, *AIP Advances*, 11, 1-15, 2021.
- Tarakka, R., Salam, N., Mochtar, A.A., Rauf, W., Ihsan, M., On the aerodynamics of rear of vehicle model with active control by blowing: computational and experimental analysis, *International Journal of Mechanical Engineering and Robotics Research*, 12(2), 84-90, 2023.
- Tarakka, R., Salam, N., Jalaluddin, Rauf, W., Ihsan, M., Aerodynamic drag reduction on the application of suction flow control on vehicle model with varied upstream velocity, *IOP Conf. Series: Materials Science and Engineering*, 1173, 1-10, 2021.
- Wang, L., Alam, M.M., Zhou, Y., Two tandem cylinders of different diameters in cross-flow: effect of an upstream cylinder on wake dynamics, *J. Fluid Mech*, 836, 5-42, 2018.
- Zhou, Q., Alam, M.H., Cao, S., Liao, H., Li, M., Numerical study of wake and aerodynamic forces on two tandem circular cylinders at  $Re = 10^3$ , *Physics of Fluids*, 31, 1-17, 2019.